AIAA 91-0494

Scattering of Sound Waves by a Compressible Vortex

T. Colonius, S.K. Lele, and P. Moin
Stanford University
Stanford, CA

29th Aerospace Sciences Meeting
January 7-10, 1991/Reno, Nevada

SCATTERING OF SOUND WAVES BY A COMPRESSIBLE VORTEX

Tim Colonius
Sanjiva K. Lele*
Parviz Moin**
Department of Mechanical Engineering
Stanford University, Stanford, CA 94305

Abstract

Scattering of plane sound waves by a compressible vortex is investigated by direct computation of the 2-d Navier-Stokes equations. Non-reflecting boundary conditions are utilized, and their accuracy is established by comparing results on different sized domains. Scattered waves are directly measured from the computations. The resulting amplitude and directivity pattern of the scattered waves is discussed, and compared to various theoretical predictions. For compact vortices (zero circulation), the scattered waves directly computed are in good agreement with predictions based on an acoustic analogy. Strong scattering at about $\pm 30°$ from the direction of incident wave propagation is observed. Back scattering is an order of magnitude smaller than forward scattering. For vortices with finite circulation refraction of the sound by the mean flow field outside the vortex core is found to be important in determining the amplitude and directivity of the scattered wave field.

1. Introduction

As a first step towards direct computations of aerodynamic sound generation in free shear flows using the Navier-Stokes equations, the scattering of plane sound waves by a compressible vortex is investigated. In a review paper by Crighton[1], the difficulties of direct computation of aeroacoustic fields are discussed. They include: the large extent of the acoustic field compared with the flow field; the small energy of the acoustic field compared to the flow; and the possibility that numerical discretization may introduce a significant sound source due to the acoustic inefficiency of low Mach number flows[1]. The vortex scattering problem is chosen to evaluate the feasibility and accuracy of the direct Navier-Stokes computation of the acoustic field along with the flow field, because of the significant amount of theoretical work on this problem available for comparison.

A nearly inviscid ($Re = u_{\theta max} L/\nu = 10^5$, where $u_{\theta max}$ is the maximum tangential velocity, L is the core radius of the vortex, and ν is the kinematic viscosity at ambient temperature) compressible vortex is irradiated with small amplitude (10^{-5} relative to the maximum vortex velocity) plane sound waves. The vortex is initially homentropic, and hence the density and pressure in the core of the vortex are lower than ambient. Several different distributions of tangential velocity with both zero and finite circulation are used[2]. Figure 1 shows a schematic drawing of the flow configuration. Plane sound waves propagating in the $+x_1$ direction are generated on the left computational boundary (see Figure 1). The scattered waves are measured directly from the simulations over the computational domain.

Two dimensionless quantities are important in determining the amplitude and directionality of the scattered wave field: the length scale ratio λ/L, where λ is the wavelength of the incident sound, and L is the core radius of the vortex; and in vortices with finite circulation, $\Gamma/(a_\infty \lambda)$, where a_∞ is the ambient sound speed. Approximate analytical solutions are reported in the literature in the case of large λ/L, using the Born approximation (see for example, Müller & Matschat[3],Howe[4], O'Shea[5], and Yates[6]), and in the case of small λ/L using ray tracing techniques (Georges[7]). The problem has been studied numerically in the case of large λ/L by Candel[8]. For vortices with finite circulation, the tangential velocity decays as $\Gamma/(2\pi r)$ where r is the distance from the vortex core. In this case, not only is sound produced by interaction of the incident wave with the vortex core, but the incident and scattered sound waves are refracted by the velocity field outside the core. The ratio $\Gamma/(a_\infty \lambda)$, which is proportional to the Mach number of the flow ($M = u_{\theta max}/a_\infty$, where $u_{\theta max}$ is the maximum tangential velocity of the vortex), controls the magnitude of the velocity field outside the core, and is therefore important in determining the magnitude of the refraction effect. For vortices with zero circulation, the total angular momentum of the flow is an invariant, and therefore a dimensionless parameter relating the total angular momentum to the

* Also with Department of Aeronautics and Astronautics, Stanford University.
** Also at NASA-Ames, Member AIAA.

core size of the vortex, the sound speed at infinity, and the wavelength of the incident sound will be important. As in the finite circulation case, this parameter will be proportional to M. Moreover, the density inhomogeneity associated with the compressible vortex also contributes to the scattering amplitude and directivity.

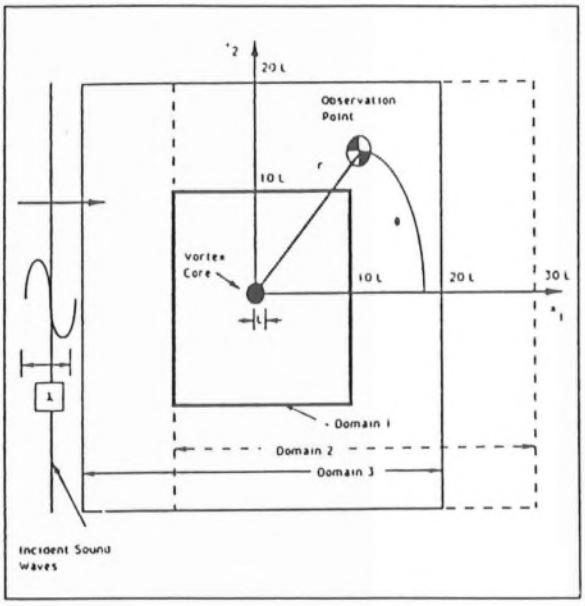

FIGURE 1. Schematic diagram of flow configuration.

In the analysis of Howe[4], the Mach number is small and the wavelength of the incident sound is much larger than the core size of the vortex, and refraction is neglected. Interaction of the incident wave with the vorticity field produces a dipole scattering cross section, with maximum scattering amplitude at $\pm 90°$ from the direction of incident sound, the scattering amplitude is zero in the forward and backward directions. In the analysis of O'Shea[5] and Yates[6], the refraction effect is included (in the Born approximation), and the scattering amplitude is found to be infinite in the forward scattering direction. This singularity is avoided by Müller & Matschat[3] by introducing a finite cut-off radius beyond which the velocity field of the vortex is ignored.

In Section 2, a brief description of the numerical method used is given. We concentrate mainly on developing boundary conditions which allow acoustic waves to propagate out of the computational domain, i.e. non-reflecting boundary conditions.

In Section 3, scattering of waves by vortices with zero circulation (and hence no refraction of sound outside the vortex core) is computed. Semi-analytical solutions are found for this case, and the results agree well with the numerical solutions. Results are also given for the scattered waves of vortices with finite circulation, with Mach number, M, ranging from .0625 to .5 and wavelength to core radius ratio from 4 to 8, Effects of refraction are investigated, and the scaling of the scattered waves is computed. The scattered field is compared with the theories described above, and to the scattering from vortices with zero circulation. The scattering of sound by the density inhomogeneity associated with the compressible vortex is also examined.

A summary of the conclusions is given in Section 4.

2. Numerical Considerations

The 2-d compressible, unsteady Navier-Stokes equations are solved numerically on the domain shown in Figure 1, which typically extends to 10 vortex core radii in each direction. 4th order accurate spatial derivatives are computed with a modified Padé scheme (Lele[9]) on a mesh of 151×151 grid points. Solutions are advanced in time using a 4th order Runge-Kutta scheme. Non-reflecting boundary conditions (Thompson[10], Poinsot & Lele[11]) are utilized. Since the velocity field of the vortex with finite circulation decays only as $1/r$, velocities at the artificial numerical boundaries are significant, and the boundary conditions must be modified to take into account the inflow and outflow of momentum, mass, and energy. At the boundary, the conservation equations are solved in characteristic form (Thompson[10]) where terms representing the amplitude of different waves crossing the boundary are isolated. These characteristic amplitudes are then specified either by computation from interior grid points via one sided differences if the wave is propagating out of the domain, or are specified independently of the interior solution for waves propagating into the domain.

In constructing one-dimensional non-reflecting boundary conditions one specifies the amplitudes of the incoming characteristic waves to be zero for all times. In the case of the vortex, the mean flow gradients are not zero at the boundary, and such boundary specifications are not appropriate. To specify the appropriate boundary conditions, we first decompose the flow at the boundary into a mean flow, and an acoustic perturbation. Since the vortex flow is irrotational outside the core, the mean flow at the boundary is essentially inviscid and steady until the viscous vortex core has spread to the boundary. Since this spreading is very slow compared to acoustical time scales, we can compute the vortex scattering well before the core has spread significantly. Therefore, the amplitudes of the incoming characteristics of the mean flow can be specified by using the gradients of the homentropic, irrotational initial

condition at the boundary. The amplitudes of the incoming characteristics of only the fluctuating acoustic part of the flow are then specified to be zero. The resulting boundary specifications involve two important approximations. First, the approximations are equivalent to assuming that mean flow varies slowly near the boundary, compared with the wavelength of the acoustic fluctuations. Secondly, the boundary conditions are strictly non- reflecting only when out-going waves propagate *normal* to the boundary. As a test of the preceding boundary conditions, the scattering from a vortex with finite circulation at $M = .25$ was computed on the "standard" domain extending to 10 core radii in each direction (labeled as Domain 1 in Figure 1), and also on a domain which extended to 30 core radii in the $+x_1$ direction (labeled as Domain 2 in Figure 1). The root mean square pressure amplitude of the scattered waves is plotted versus the angle from the $+x_1$ axis for both domains at $r = 10L$ in Figure 2. The agreement between the two curves is good, the maximum difference between the scattering amplitudes for the smaller and larger domains being about 5%.

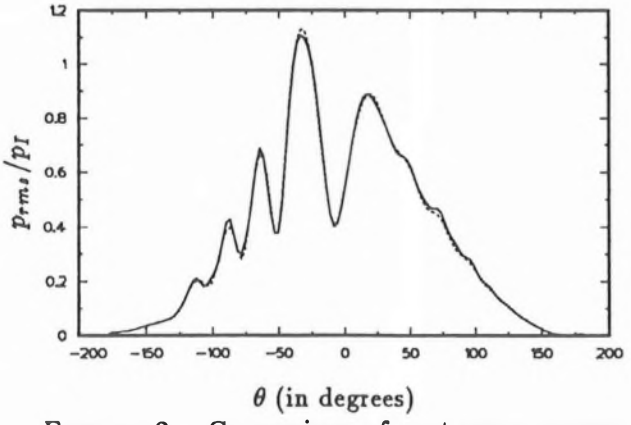

FIGURE 2. Comparison of root mean square pressure level of scattered wave, normalized by the amplitude of the incident waves, between simulations on different sized domains: —— Domain 1; ---- Domain 2. See Figure 1 for domain sizes.

For this particular flow, the assumption of normal waves at the boundary (1-D characteristics) is accurate, since the waves strike the boundary with nearly normal incidence. We find that these boundary conditions are not adequate in general, when waves strike the computational boundaries at oblique angles. Improvements for this case will be described in a forthcoming publication.

3. Results and Discussion

3.1 Scattering from a Vortex with Zero Circulation- Computations and Analysis

The scattering of plane sound waves by the homentropic vortex with zero circulation is computed. The distribution of tangential velocity is taken to be:

$$u_\theta = Mr\exp(\frac{1-r^2}{2}), \tag{1}$$

the radial velocity is zero, and the pressure is given by solving:

$$\frac{\partial p}{\partial r} = \rho\frac{u_\theta^2}{r}, \tag{2}$$

The velocity profile is scaled such that the maximum tangential velocity occurs at $r/L = 1$ (this fixes the relation between the Mach number, M, and the total angular momentum of the flow). This flow satisfies the inviscid equations. Incident waves are generated at the boundary of the domain, and are allowed to propagate through the entire computational domain. Statistics of the scattered field are then gathered over many periods of the incident waves. The viscous decay of the vortex over this time period is accounted for by computing a vortex without incident sound, and subtracting the result from the vortex with incident sound. The resulting wave field is verified to be monochromatic at the frequency of the incident waves, to a very high degree of accuracy. Viscous effects on the waves are negligible since $(\omega\lambda^2)/\nu \gg 1$, where ω is the frequency of the waves.

The root mean square pressure level of the scattered waves is plotted as a function of observation angle (defined in Figure 1) for increasing values of r/λ in Figure 3, at $M = .125$. The pressure is normalized by the amplitude of the incident wave, and $(\lambda/r)^{1/2}$. The collapse of the curves for the larger values of λ/r plotted indicates that the far-field asymptotic behavior has been reached. The factor of $(\lambda/r)^{1/2}$ arises from the decay of the scattered waves in two- dimensions (see equation 11). The asymptotic directivity is strongly peaked at $\pm 30°$ from the direction of incident propagation ($\theta = 0$). Back scattering is an order of magnitude smaller than in the forward direction. There is a slight asymmetry in the directivity with respect to the direction of incident propagation, the peak at $-30°$ being slightly higher than the peak at $+30°$, when the vortex spins clockwise (if the sense of the circulation is reversed, the directivity pattern is reflected about $\theta = 0$).

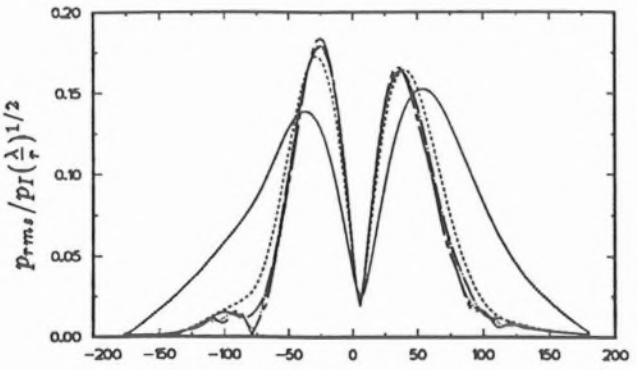

FIGURE 3. Root mean square pressure level of scattered waves, normalized by amplitude of incident wave and $(\frac{\lambda}{r})^{1/2}$. $M = .125$, $\frac{\lambda}{L} = 4$: ——— $\frac{r}{\lambda} = .5$; ---- $\frac{r}{\lambda} = 1.0$; —·— $\frac{r}{\lambda} = 1.5$; ····· $\frac{r}{\lambda} = 2.0$; —·— $\frac{r}{\lambda} = 2.5$.

In order to determine the accuracy of the computed scattered waves, it is desirable to calculate the far-field sound using an acoustic analogy (e.g. Lighthill's Equation) and compare it to the sound measured directly in the solutions to the full equations, where source terms in the acoustic analogy are measured in the near field of the computations. Agreement between the two results would indicate sufficient resolution of the sound sources, and rule out numerical discretization as a source of sound. Since the mean flow field for the vortex with finite circulation decays slowly $(1/r)$, the source terms for an acoustic analogy would decay only algebraically in the far-field. This fact coupled with the truncation of the computational domain prevents the determination of the source terms for the computations of vortices with finite circulation. In the present case, the mean flow decays exponentially fast away from the vortex core, with ambient conditions rapidly approached near the computational boundaries, and source terms for acoustic analogy can be computed.

Linearizing the 2-d Euler equations about the mean flow, and isolating terms which decay to zero outside the core on the right hand side produces a wave equation for the density perturbation:

$$\frac{\partial^2 \rho'}{\partial t^2} - \nabla^2 \rho' = S(x_1, x_2, t), \tag{3}$$

where S is the source term which includes products of the mean field (which decays exponentially fast outside the vortex core) and the perturbation density, and velocities. S is given by:

$$\begin{aligned} S(x_1,x_2,t) = {} & \frac{\partial \rho'}{\partial x_2}\frac{\partial a_0^2}{\partial x_2} + \frac{\partial \rho'}{\partial x_1}\frac{\partial a_0^2}{\partial x_1} - \frac{\partial \rho'}{\partial t}(\frac{\partial u_0}{\partial x_1} + \frac{\partial v_0}{\partial x_2}) \\ & - u_0\frac{\partial^2 \rho'}{\partial x_1 \partial t} - v_0\frac{\partial^2 \rho'}{\partial x_2 \partial t} + (a_0^2 - 1)\nabla^2 \rho' \\ & + \frac{\partial}{\partial x_1}(\rho_0 u_0 \frac{\partial u'}{\partial x_1} + \rho_0 u' \frac{\partial u_0}{\partial x_1} \\ & + \rho_0 v_0 \frac{\partial u'}{\partial x_2} + \rho_0 v' \frac{\partial u_0}{\partial x_2} - \frac{\rho'}{\rho_0}\frac{\partial p_0}{\partial x_1}) \\ & + \frac{\partial}{\partial x_2}(\rho_0 u_0 \frac{\partial v'}{\partial x_1} + \rho_0 u' \frac{\partial v_0}{\partial x_1} \\ & + \rho_0 v_0 \frac{\partial v'}{\partial x_2} + \rho_0 v' \frac{\partial v_0}{\partial x_2} - \frac{\rho'}{\rho_0}\frac{\partial p_0}{\partial x_2}) \end{aligned} \tag{4}$$

where u and v are the velocities in the x_1 and x_2 directions, the subscript 0 refers to the (steady) mean vortex flow, and the prime refers to the perturbations. The quantities in equations (3) and (4) are made dimensionless by referring velocities to the ambient sound speed, lengths to the core radius of the vortex, and density to the ambient density.

Since the waves are monochromatic,

$$f' = Real(\hat{f}\exp(-i\omega t)), \tag{5}$$

where f' is any of u',v', and ρ', and $\omega = (2\pi a_\infty)/\lambda$. Using (5) in (4),

$$(\nabla^2 + \omega^2)\hat{\rho} = -\hat{S}. \tag{6}$$

The scattered waves are defined by

$$\hat{f} = \hat{f}_{sc} + \hat{f}_I, \tag{7}$$

where the subscript sc refers to the scattered wave and the subscript I refers to the incident wave. Since the incident wave satisfies (6) with $\hat{S} = 0$,

$$(\nabla^2 + \omega^2)\hat{\rho}_{sc} = -\hat{S}. \tag{8}$$

Which has the solution

$$\hat{\rho}_{sc} = \int_{-\infty}^{\infty}\int_{-\infty}^{\infty} \frac{i}{4}\hat{S}(\mathbf{x}')H_0^{(1)}(|\mathbf{x} - \mathbf{x}'|\omega)dx_1'dx_2', \tag{9}$$

where $H_0^{(1)}$ is the zeroth order Hankel function.

The source term $\hat{S}$ is evaluated from the results of the computations, and the integral in equation (9) is performed numerically, over the computational domain. The resulting root mean square density of the scattered waves ($\rho_{rms} = \sqrt{1/2|\hat{\rho}|^2}$) is plotted versus the observation angle in Figure 4 for $r = 2\lambda$. Also plotted is the value of ρ_{rms} measured directly from the computations. The curves agree to within a few percent, and we conclude that numerical discretization is not acting as a significant source of sound.

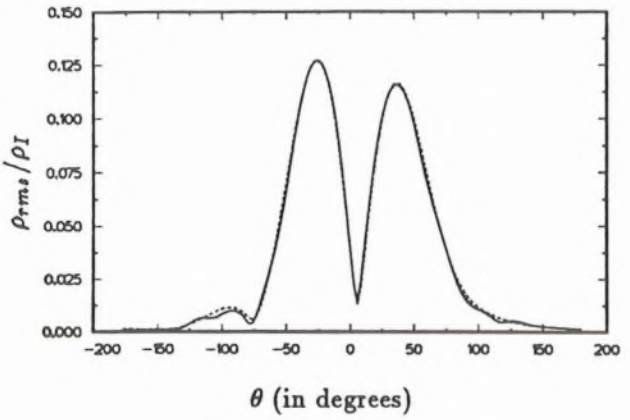

FIGURE 4. Comparison of root mean square density of scattered wave. —— Directly Computed; ---- Computed from Equation (9) with $\hat{S}$ measured from computations.

The source term $\hat{S}$ can also be evaluated in the first scattering approximation, where the scattered waves are assumed to be much smaller than the incident waves. In this case $\hat{S}$ can be evaluated without the computational results. The resulting root mean square density of the scattered waves are compared to the value computed with the source term measured from the computations in Figure 5. Since the problem is linear, the difference between the two curves represents the interaction of the scattered wave with the mean vortex flow. The directivity pattern in the first scattering approximation is symmetrical, and is exactly zero in the forward direction. Hence the asymmetry in the directivity pattern, as well as the finite scattering in the forward direction are attributed to interaction of the scattered wave with the mean flow field.

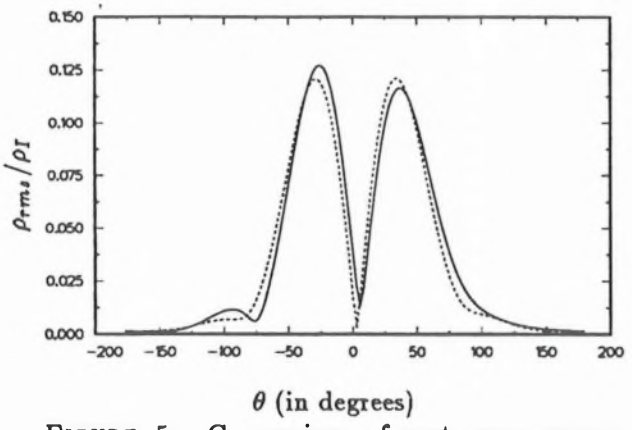

FIGURE 5. Comparison of root mean square density of scattered wave. —— Computed from Equation (9) with $\hat{S}$ measured from computations; ---- Computed from Equation (9), in the first scattering approximation.

3.2 Scattering from Vortices with Finite Circulation

Vortices with finite circulation are modeled with the Oseen tangential velocity profile:

$$u_\theta = \frac{\Gamma}{2\pi r}\left(1 - \exp(-1.256431(r/L)^2)\right), \qquad (10)$$

where the profile has been scaled such that the maximum tangential velocity occurs at $r/L = 1$. The scattered waves are directly computed in the same manner discussed in Section 3.1. Figure 6 shows contours of the root mean square pressure level of the scattered wave for $\Gamma/(a_\infty \lambda) = .27$ ($M = .125$) and $\lambda/L = 4$. As in the zero circulation case, there is preferred scattering in the forward direction, and the scattering is asymmetrical with respect to the direction of incident propagation. The maximum scattering occurs at about -30 degrees from the direction of incident propagation (the vortex spins clockwise). Scattering in the backward direction is again at least an order of magnitude smaller than in the forward direction.

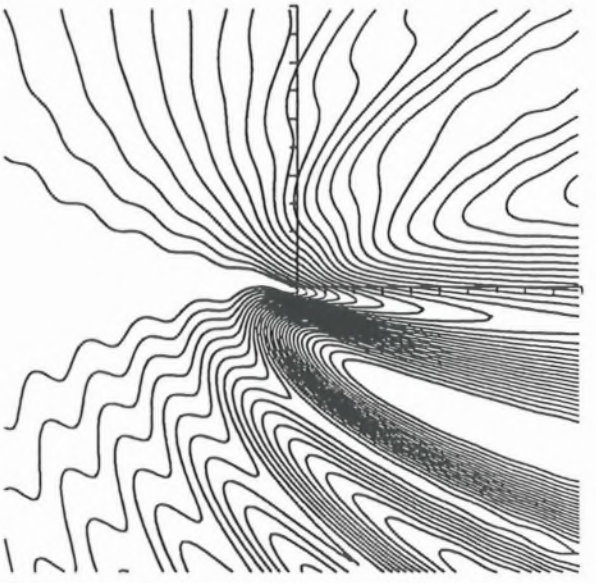

FIGURE 6. Iso-contours of the root mean square pressure level of the scattered wave. Normalized by amplitude of incident wave. Contour levels: Minimum = .08; Maximum = 1.12; Increment = .04.

In Figure 7, the root mean square pressure scattering amplitude at $r = 2.5\lambda$ is plotted versus the angle from the direction of incident propagation, for $\lambda/L = 4$, and $\Gamma/(a_\infty \lambda)$ ranging from .14 to 1.1. A trend towards more asymmetrical cross sections as the parameter $\Gamma/(a_\infty \lambda)$ is increased is clearly discernible, and the oscillations in the bottom half plane of the cross section ($-180° < \theta < 0°$) become more pronounced.

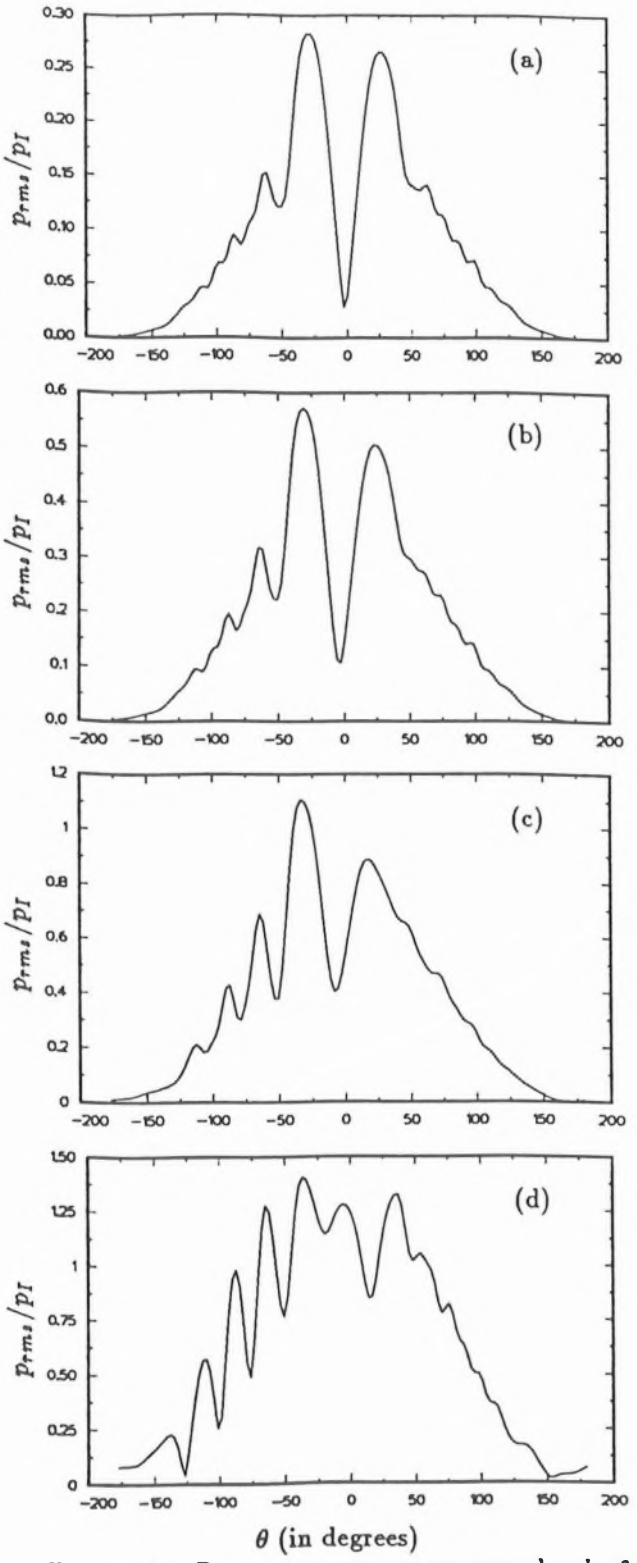

FIGURE 7. Root mean square pressure level of scattered wave at $r = 2.5\lambda$. a) $\frac{\Gamma}{a_\infty \lambda} = .14$ b) $\frac{\Gamma}{a_\infty \lambda} = .27$ c) $\frac{\Gamma}{a_\infty \lambda} = .55$ d) $\frac{\Gamma}{a_\infty \lambda} = 1.1$.

This is evidently an effect of refraction of the incident and generated sound by the flow outside the vortex core, with the oscillations resulting from interference effects. There were no such oscillations in the cross sections from vortices with zero circulation (Figure 3), where refraction by the mean flow is insignificant outside the core. At the lowest $\Gamma/(a_\infty \lambda)$ (Figure 7*a*), the cross section is more nearly symmetric about the forward scattering direction, and as $\Gamma/(a_\infty \lambda)$ is reduced, the scattering in the forward direction appears to go to zero.

According to aeroacoustic theory[3,4,5,6], in the far field the root mean square pressure level should scale as

$$p_{rms} \sim p_I \frac{\Gamma}{a_\infty \lambda} \left(\frac{\lambda}{r}\right)^{1/2}. \tag{11}$$

In Figure 8, the root mean square scattered pressure is normalized by the quantity on the right hand side of equation (11), and plotted at $r/\lambda = 2.5$, for various values of $\Gamma/(a_\infty \lambda)$ and λ/L. As $\Gamma/(a_\infty \lambda)$ is reduced and λ/L is increased, the curves collapse and the scaling appears to hold.

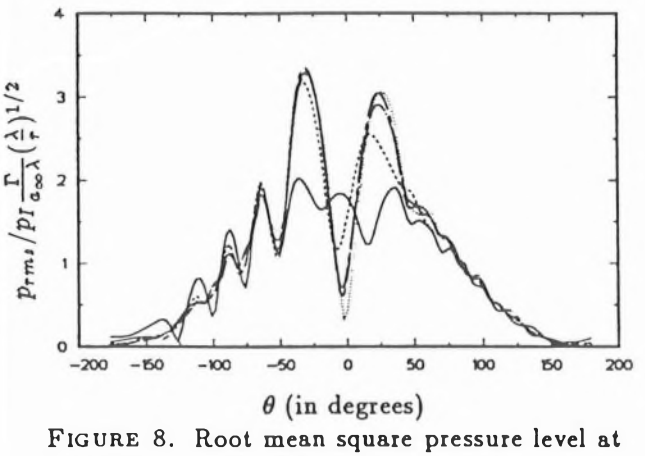

FIGURE 8. Root mean square pressure level at $r = 2.5\lambda$ normalized by right hand side of equation (2): —— $\frac{\Gamma}{a_\infty \lambda} = 1.1$, $\frac{\lambda}{L} = 4$; ---- $\frac{\Gamma}{a_\infty \lambda} = .55$, $\frac{\lambda}{L} = 4$; —·— $\frac{\Gamma}{a_\infty \lambda} = .27$, $\frac{\lambda}{L} = 4$; ····· $\frac{\Gamma}{a_\infty \lambda} = .14$, $\frac{\lambda}{L} = 4$; —·· $\frac{\Gamma}{a_\infty \lambda} = .27$, $\frac{\lambda}{L} = 8$.

In Figure 9, the scattered pressure level is plotted for different values of r/λ, with $\Gamma/(a_\infty \lambda)$ and λ/L fixed. The curves collapse well away from the forward scattering direction ($\theta = 0$). Near the forward direction, however, the peak scattering does not scale like $(\lambda/r)^{1/2}$. The same curves are plotted in Figure 10, but the pressure is not normalized by the factor $(\lambda/r)^{1/2}$. In fact, Figure 10 shows that the peak scattering is very nearly constant in r/λ. This lack of scaling with λ/r is attributed to refractive effects by the mean flow field, as will be discussed in Section 3.3. Figure 9 also shows that the oscillations in the cross section becomes more

pronounced further from the vortex core (at larger r/λ), which supports the claim that they are caused by refraction effects.

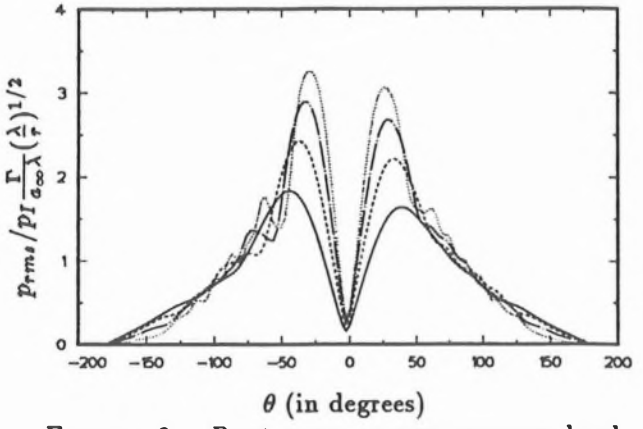

FIGURE 9. Root mean square pressure level normalized by right hand side of equation (2). $\frac{\Gamma}{a_\infty\lambda} = .14$, $\frac{\lambda}{L} = 4$: ——— $\frac{r}{\lambda} = 1$; ---- $\frac{r}{\lambda} = 1.5$; —·— $\frac{r}{\lambda} = 2$; ····· $\frac{r}{\lambda} = 2.5$.

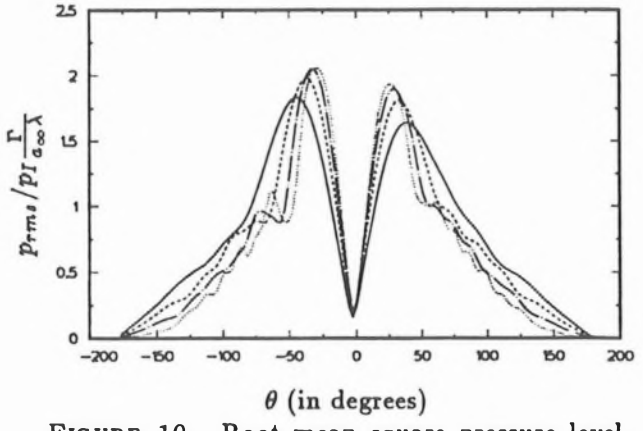

FIGURE 10. Root mean square pressure level normalized by $p_I\frac{\Gamma}{a_\infty\lambda}$. $\frac{\Gamma}{a_\infty\lambda} = .14$, $\frac{\lambda}{L} = 4$: ——— $\frac{r}{\lambda} = 1$; ---- $\frac{r}{\lambda} = 1.5$; —·— $\frac{r}{\lambda} = 2$; ····· $\frac{r}{\lambda} = 2.5$.

The compressible vortex has additional scattering effects due to the local change in the speed of sound, produced by the density inhomogeneity associated with the core. To determine the magnitude of this effect, the scattering of plane waves by a density inhomogeneity alone (without the vortex velocity field) is computed. The density distribution is taken to be the same as that of the homentropic vortex at $\Gamma/(a_\infty\lambda) = 1.1$, where the Mach number is .5 and the density change is most pronounced. The scattering is symmetric in this case, and it is found that the scattering amplitude is an order of magnitude smaller than scattering from the vortex at the same conditions. This suggests that the density inhomogeneity associated with the compressible vortex (up to modest Mach numbers), is not very important in determining the amplitude of the scattered waves. This result is echoed in the analysis of Müller & Matschat[3] where the local change in the sound speed produced by the vortex flow is found to be proportional to $(\Gamma/(a_\infty\lambda))^2$.

3.2 Comparison with Analytical Theories

Although the amplitude of the scattered waves are found to scale with the amplitude of the incident wave and $\Gamma/(a_\infty\lambda)$, as predicted by the aeroacoustic theories[3,4,5,6], the directivity pattern shown in Figure 9 does not agree with the predicted directivity patterns, and maximum root mean square pressure does not scale with $(\lambda/r)^{1/2}$. The scattering intensity goes to zero in both the forward and backward directions, but the peak scattering angles are much closer to the forward direction ($\pm 30°$), than the dipole pattern predicted by Howe[4], where the maximum occurs at $\pm 90°$. According to Yates[6], the result of Howe[4] is incomplete, and an additional term needs to be retained to yield a quadrupole distribution, which is also not observed in the computations. Although the intensity is peaked *around* the forward scattering direction, the scattering does go to zero in the forward direction in contrast to the infinite scattering predicted[5,6]. If a finite cut-off radius beyond which the vortex velocity is ignored is included[3], the scattering once again goes to zero in the forward direction, but the predicted directivity is again a quadrupole.

We will now analyze these discrepancies in more detail. There are two important differences between the theories and the computations:

(i) The core vorticity distributions assumed by the analysis[3,4,5,6] are different from the computations which assume a Gaussian vorticity distribution.

(ii) Incident plane waves are introduced as $x_1 \to -\infty$ in the analysis[3,4,5,6]. Due to the truncated domain in the computation, the incident waves are assumed to be planar at $x_1 = -2.5\lambda$, and therefore refraction effects of the incident waves from $x_1 \to -\infty$ to $x_1 = -2.5\lambda$ are ignored.

To investigate the effect of (i) in the directivity pattern, a computation was performed with a vorticity distribution similar to the "tophat" distribution used in the analysis[4]. Since a discontinuity in the vorticity is not permissible in the computations, we simulate the "tophat distribution" with a vorticity which decays as $\exp(-r^n)$, where $n = 6$ ($n = 2$ for the Gaussian distribution). For large n, this distribution approaches the "tophat" distribution. The root mean square scattered

pressure level at $r/\lambda = 2.5$ for the $n = 6$ and $n = 2$ vorticity distributions are compared in Figure 11. There is nearly no difference in the two, and apparently (i) cannot explain the discrepancy between the analysis of Howe[4] (with or without the correction by Yates[6]) and the computations. This lack of sensitivity to the core profiles is in accord with the results of Yates[6], who has considered scattering from vortices with a variety of core vorticity distributions (where refraction effects are retained and the result is singular in the forward direction). Although there are quantitative differences in the resulting scattering cross sections, qualitatively similar directivity patterns are observed[6].

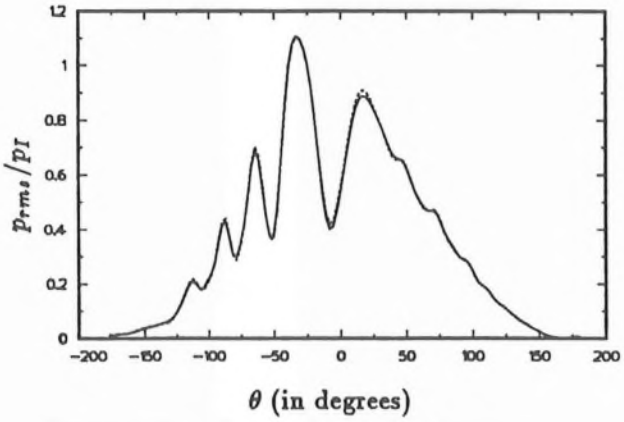

FIGURE 11. Comparison of root mean square pressure level of scattered wave between computations with different vorticity distributions: —— Gaussian vorticity; ---- "tophat" vorticity.

Item (ii) above is potentially more serious. Since refraction effects are neglected by Howe[4], the incident waves in the analysis remain planar until interacting with the core. Since the waves are assumed to be planar at $r = -2.5\lambda$, and λ/L is always larger than 1 in the computations, we conclude that (ii) cannot be responsible for the discrepancy with the results of Howe[4]. Theories which include the long range refractive effects of the mean flow predict singular results in the forward direction. This is interpreted to mean that the basic scattering approximation (Born approximation) is not valid in the forward scattering direction.[5,6] Apparently the long range refraction of the incident waves may not be small, even in the limit of small $\Gamma/(a_\infty \lambda)$. In fact, the source term (equation (4)) for the acoustic analogy will decay like $1/r$ for vortex flows with finite circulation, due to the convective terms which have been included in the source term (the fourth and fifth terms on the right hand side of equation (4))). Hence the integral in equation (9) is not well defined, and therefore the scattered waves are not required to decay as $(\lambda/r)^{1/2}$ in the far-field. A proper analytical treatment of the finite circulation problem should retain convective terms in the wave operator on the left hand side of equation (5).

To further investigate refraction effects, a computation at $\Gamma/(a_\infty \lambda) = .55$ was conducted on a larger domain which extended to 20 vortex core radii in each direction (labeled as Domain 3 in Figure 1). The incident sound waves generated at the boundary therefore refract over distances twice as long as in the previous computations, before impinging on the vortex core. The scattering amplitude is plotted versus the observation angle at $r = 2.5\lambda$ in Figure 12, for both the larger and smaller domains. The scattering amplitude is everywhere greater for the larger domain, especially in the backward direction.

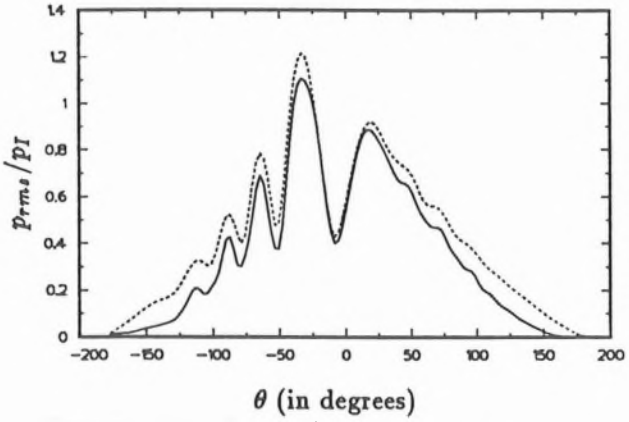

FIGURE 12. Comparison of root mean square pressure level of scattered wave between simulations on different sized domains: —— Domain 1; ---- Domain3. See Figure 1 for domain sizes.

Therefore, it is perhaps more appropriate to qualitatively compare the computed results to a slightly different problem, that of the scattering from a line source of sound, located at some finite distance from the vortex, which has been studied by O'Shea[5] and Yates[6]. The resulting directivity pattern given by Yates[6] has many feature in common with the computed directivity patterns shown in Figure 4: asymmetry with respect to the forward scattering direction; maximum scattering at about -30 degrees from the forward direction (when the vortex spins clockwise); and little scattering in the backward direction.

4. Summary

The scattering of plane sound waves by a compressible vortex is studied using direct computation of the 2-d Navier-Stokes equations. Non-reflecting boundary

conditions developed for this problem are tested by increasing the size of the computational domain by a factor of 2 in each direction. Good agreement between the results from the larger and smaller domains is observed (to within 5%).

Scattering is peaked at $\pm 30°$ around the direction of incident propagation. The scattering is asymmetrical, owing to interaction of the scattered waves with the mean field. Scattering the the backward direction is an order of magnitude smaller than in the forward direction.

For compact vortices where the tangential velocity decays exponentially fast outside the core (zero circulation), the scattering directly measured from the computations agrees well with predictions found by solving an acoustic analogy (a wave equation derived from linearized Euler equations), where the source terms in the wave equation are determined by the computations, indicating a good numerical approximation of the sound sources–numerical discretization does not act as a source of sound in the computations.

For vortices with finite circulation, the root mean square scattered waves scale as

$$p_{rms} \sim p_I \frac{\Gamma}{a_\infty \lambda},$$

in the limit of small $\Gamma/(a_\infty \lambda)$ and large λ/L. Furthermore, as $\Gamma/(a_\infty \lambda)$ is reduced, the cross section becomes more symmetrical, and the scattering goes to zero in the incident direction. The directivity pattern observed for vortices with finite circulation do not agree well with theoretical predictions[3,4,5,6], owing to important effects of refraction of the incident and generated waves by the slowly $1/r$ decaying mean velocity of the vortex.

Acknowledgements

This work was supported by the Office of Naval Research.

REFERENCES

[1] Crighton, D.G. 'Goals for computational aeroacoustics.' Computational Acoustics: Algorithms and Applications. Elsevier Science Publishers B.V., IMACS, 1988.

[2] Colonius, T., Lele, S.K. & Moin, P. 'The free compressible viscous heat conducting vortex.' 1990. *Submitted to J. Fluid Mech.*

[3] Müller, E.A. & Matschat, K.R. 'The scattering of sound by a single vortex and by turbulence.' *Tech. Rep. Max-Planck-Inst. für Strömungsforschung, Göttingen.*, 1959.

[4] Howe, M.S., 'Contributions to the theory of aerodynamic sound, with application to excess jet noise and theory of the flute.' *J. Fluid Mech.*, 71:625-673, 1975.

[5] O'Shea, S., 'Sound Scattering by a Potential Vortex.'*J. Fluid Mech.*, 43:109-116, 1975.

[6] Yates, J.E., 'Application of the Bernoulli Enthalpy Concept to the Study of Vortex Noise and Jet Impingement Noise.' NASA Contractor Report 2987, 1978.

[7] Georges, T.M. 'Acoustic Ray Paths through a Mode Vortex with a Viscous Core.' *J. Acoust. Soc. Am.*,51:206-209, 1972.

[8] Candel, S.M. 'Numerical solution of wave scattering problems in the parabolic approximation.' *J. Fluid Mech.*,33:465-507, 1980.

[9] Lele, S.K. 'Compact finite difference schemes with spectral-like resolution.' CTR Manuscript 107, 1990, *Submitted to J. Comput. Phys.*

[10] Thompson, K.W. 'Time Dependant Boundary Conditions for Hyperbolic Systems.' *J. Comput. Phys.*, 68:1-24, 1987.

[11] Poinsot, T.J. & Lele, S.K. 'Boundary conditions for direct simulations of compressible viscous reacting flows.' CTR Manuscript 102, 1989, *Submitted to J. Comput. Phys.*